Geomechanics and Engineering, *Vol. 9, No. 3 (2015) 313-328*
DOI: http://dx.doi.org/10.12989/gae.2015.9.3.313

CPT-based *p-y* analysis for mono-piles in sands under static and cyclic loading conditions

Garam Kim, Doohyun Kyung, Donggyu Park and Junhwan Lee *

Department of Civil and Environmental Engineering, Yonsei University, 134 Shinchon-dong, Seodaemun-gu, Seoul 120-749, Republic of Korea

(*Received August 07, 2014, Revised January 27, 2015, Accepted April 25, 2015*)

Abstract. In the present study, a CPT-based *p-y* analysis method was proposed for offshore mono-piles embedded in sands. Static and cyclic loading conditions were both taken into account for the proposed method. The continuous soil profiling capability of CPT was an important consideration for the proposed method, where detailed soil profile condition with depth can be readily incorporated into the analysis. The hyperbolic function was adopted to describe the non-linear *p-y* curves. For the proposed hyperbolic *p-y* relationship, the ultimate lateral soil resistance p_u was given as a function of the cone resistance, which is directly introduced into the analysis as an input data. For cyclic loading condition, two different cyclic modification factors were considered and compared. Case examples were selected to check the validity of the proposed CPT-based method. Calculated lateral displacements and bending moments from the proposed method were in good agreement with measured results for lateral displacement and bending moment profiles. It was observed the accuracy of calculated results for the conventional approach was largely dependent on the selection of friction angle that is to be adopted into the analysis.

Keywords: *p-y* curve; cone penetration tests; laterally loaded piles; beam on elastic foundation; lateral load transfer analysis

1. Introduction

Mono-piles are often used for offshore structures, such as offshore wind turbines and jetties, with water depths shallower than around 30 to 40 m. The lateral load response is key design consideration for offshore mono-piles as waves and winds are predominant load components (API 2010, DNV 2013). For offshore conditions, the identification of design soil parameters becomes challenging as the conventional sampling- and testing-based procedure represents higher degree of experimental uncertainties with limited reliability of estimated soil parameters. This has led that the application of in-situ testing methods is preferred and regarded particularly effective for offshore foundation design (Titi *et al*. 2000, Tumay and Kurup 2001, Lee and Randolph 2011).

For laterally loaded piles, it is important to ensure that induced lateral displacements upon loading are within a certain tolerable limit for a given safety margin. For the displacement analysis of laterally loaded piles, the continuum-based numerical analysis or simplified beam-on-elastic

*Corresponding author, Professor, E-mail: junlee@yonsei.ac.kr

http://www.techno-press.org/?journal=gae&subpage=7 ISSN: 2005-307X (Print), 2092-6219 (Online)

foundation (BEF) approach has been often used in practice (Winkler 1867, Matlock and Reese 1960, Reese *et al*. 1974). In the BEF approach, soils are assumed as a series of discrete linear or non-linear elastic springs for which load responses are characterized by the *p-y* curve that defines the shape and magnitude of load-displacement relationship. As the *p-y* curve changes with stress state, it shows depth-dependent variation. Although the BEF approach using the *p-y* curve may be less rigorous than the full numerical analysis, it has been widely adopted in practice due to the simplicity and reasonableness of calculated results.

The application of CPT results has long been explored for characterizing various soil properties including elastic modulus and strength (Robertson and Campanella 1983, Rix and Stokoe 1991, Lee *et al*. 2008). There have also been several cases where in-situ testing methods, such as pressuremeter test (PMT) and dilatometer test (DMT), were applied to define the *p-y* curves (Briaud *et al*. 1985, Robertson *et al*. 1989, Gabr *et al*. 1994). Less attention has been given to the cone penetration test (CPT), probably due to the different loading directions between the vertically penetrating cone and laterally loaded piles. It has been well recognized that the cone resistance is essentially governed by the horizontal effective stress rather than the vertical effective stress (Schnaid and Houlsby 1991, Lee and Salgado 1999). It was however quite recently recognize that the cone resistance can be directly correlated to the lateral load responses of piles (Dyson and Randolph 2001, Suryasentana and Lehane 2014, Lee *et al*. 2010). This indicates that the applicability of CPT can be further enhanced for cases of laterally loaded piles. As current design practice for offshore foundation is still largely based on the "property-based" approach, an improvement of design methodology with direct application of in-situ test results is desired for more effective and feasible design process and sustainable construction of offshore energy infrastructures.

In this study, a CPT-based *p-y* analysis method is proposed applicable for offshore piles embedded in sands. Both static and cyclic loading conditions are addressed in the proposed method. The continuous profiling capability of CPT is an important consideration for the proposed method as well as the non-linear characteristics of *p-y* curve. In the proposed CPT-based *p-y* analysis method, detailed depth variation of soil layer profiles can be readily incorporated into the analysis by directly importing CPT results. The effects of soil layering and property variation on the *p-y* analysis are examined in comparison to the conventional *p-y* analysis method.

2. *p-y* analysis for piles in sands

2.1 Methods of p-y curve

The beam-on-elastic foundation (BEF) model is a common approach that is used to estimate and analyze the lateral load response of piles including lateral displacements and bending moments induced upon loading. In this approach, soils are assumed as a series of elastic springs with load-displacement characteristics defined by the *p-y* curves that are either linear or non-linear (Matlock 1970, Reese *et al*. 1975, API 2010, Franke and Rollins 2013). For piles in sands, the methods proposed by Reese *et al*. (1974) and API (2010) have been popular and adopted in various design specifications for offshore structures (Pando *et al*. 2006, API 2010, DNV 2013).

Reese *et al*. (1974) proposed a *p-y* curve based on the results from the full-scale lateral pile load tests. In this method, the *p-y* curve is sub-divided into different zones indicating the initial elastic, intermediate and plastic states, as described in Fig. 1(a). The ultimate lateral soil resistance is

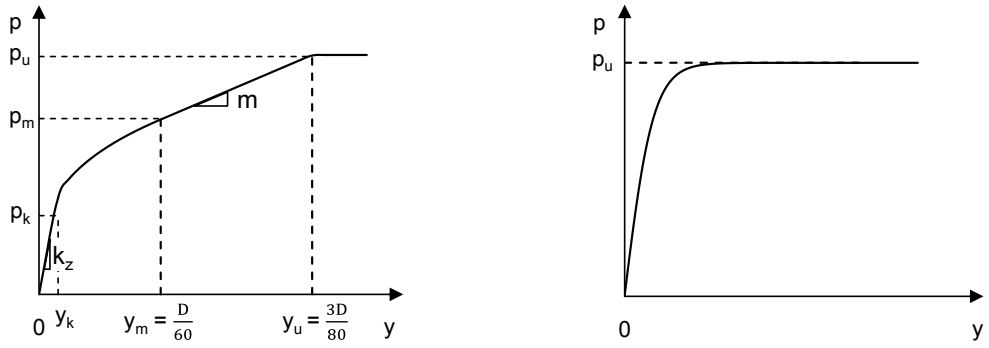

(a) Reese *et al*. (1974) (b) API (2010)

Fig. 1 Characteristic shapes of *p-y* curves for sand

assumed to be mobilized at large pile deflection equal to 3 times pile diameter divided by 80 (3D/80) from which the *p-y* curve shows flat segment. The ultimate lateral soil resistance in this method is defined as the following two equations

$$p_{ut} = A\gamma z\left[\frac{K_0 z\tan\phi\sin\beta}{\tan(\beta-\phi)\cos\alpha}+\frac{\tan\beta}{\tan(\beta-\phi)}(D+z\tan\beta\tan\alpha)\right.$$
$$\left.+K_0 z\tan\beta(\tan\phi\sin\beta-\tan\alpha)+K_a D\right] \tag{1}$$

$$p_{ut} = AD\gamma z\left[K_a(\tan^8\beta-1)+K_0\tan\phi\tan^4\beta\right] \tag{2}$$

where A = empirical adjustment parameter given as a function of depth; K_0 = coefficient of lateral earth pressure at rest = 0.4; K_a = coefficient of active earth pressure; γ = unit weight of soil; D = pile diameter; z = depth; ϕ = internal friction angle of soil; $\alpha = \phi/2$; and $\beta = 45 + \phi/2$. The ultimate lateral soil resistance p_u is given as a smaller one of p_{ut} and p_{ud}.

The *p-y* curve method given in API (2010) is defined by a single hyperbolic tangential function given as the following equation

$$p = \eta\cdot A\cdot p_u\cdot\tanh\left[\frac{kz}{\eta\cdot A\cdot p_u}y\right] \tag{3}$$

where η = pile shape factor = 1 for circular shape; A = empirical adjustment factor = $[3 - 0.8(z/D)] \geq 0.9$ for static loading and 0.9 for cyclic loading; p_u = ultimate lateral resistance; k = initial modulus of subgrade reaction; and z = depth. Fig. 1(b) shows the *p-y* curve of Eq. (3) by API (2010).

2.2 p-y curves using CPT results

Recent development for the *p-y* curve methods has been mainly focused on the modification or development of the *p-y* function that fits better to actual soil behavior (Reese 1997, McGann *et al*. 2011, Franke and Rollins 2013, Khalili-Tehrani *et al*. 2014, Chang and Hutchinson 2013). While there have been several cases for the applications of in-situ test results into the *p-y* methods

(Briaud *et al*. 1985, Robertson *et al*. 1989, Gabr *et al*. 1994, Haldar and Babu 2009), less attention has been given to the application of cone penetration test (CPT) due to the different loading mechanisms between vertically penetrating cone and laterally loaded piles. However, the cone resistance is also governed by the horizontal effective stress indicating that it may also be mechanically correlated to lateral pile load responses (Schnaid and Houlsby 1991, Lee *et al*. 2010).

Although fewer cases were addressed, certain progress has been made for the development of the *p-y* analysis methods using CPT results. These include the methods proposed by Novello (1999), Dyson and Randolph (2001) and Suryasentana and Lehane (2014), for all of which the *p-y* curves are defined using certain functional expressions with soil unit weight (γ), pile diameter (D), depth (z), and cone resistance (q_c) as model parameters. These *p-y* curves are given by

$$p = 2 \cdot D \cdot (\gamma' z)^{0.33} \cdot q_c^{0.67} \cdot \left(\frac{y}{D}\right)^{0.5} \tag{4}$$

$$\frac{p}{\gamma' D^2} = 2.7 \cdot (F_1 + F_2) \cdot \left(\frac{q_c}{\gamma' D}\right)^{0.72} \cdot \left(\frac{y}{D}\right)^{0.58} \tag{5}$$

$$\frac{p}{\gamma' D^2} = 2.7 \cdot \left(\frac{q_c}{\gamma' z}\right)^{0.67} \cdot \left(\frac{z}{D}\right)^{0.75} \cdot \left[1 - \exp\left(-6.2 \cdot \left(\frac{z}{D}\right)^{-1.2} \cdot \left(\frac{y}{D}\right)^{0.89}\right)\right] \tag{6}$$

where γ' = unit weight of soil; z = depth from soil surface; q_c = cone resistance; D = pile diameter, and F_1 and F_2 = modification factors for installation method where $z \leq 4D$. Note that Eqs. (4) and (6) contain the depth term z, which represents increasing vertical effective stress when combined with soil unit weight while the effect of horizontal stress that is required to define overall confining stress level of soils is not explicitly included.

The *p-y* functions of Eq. (4) by Novello (1999) and Eq. (5) by Dyson and Randolph (2001) were obtained experimentally using the results from centrifuge tests while Eq. (6) by Suryasentana and Lehane (2014) was established using the results from the finite element analyses. Both cases of Eqs. (4) and (5) were developed based on the data fitting process by double integrating and differentiating bending moment profiles of the results obtained experimentally. Eq. (6) was derived by the power law relationship and exponential relationship from three-dimensional finite element analyses.

3. Proposed CPT-based *p-y* curve analysis

3.1 Derivation of hyperbolic p-y function

The conventional *p-y* curve methods are subjected to the inherent limitation in that, as reported in FHWA (Pando *et al*. 2006), the soil is idealized as a series of independent elastic springs and thus the continuous nature of the soil is not explicitly modeled. It is also difficult to evaluate appropriate *p-y* modulus as it varies with depth due to changes in soil and stress conditions. The discrete nature of elastic springs in the *p-y* analysis can be compensated by introducing a continuous CPT profile directly into the analysis and reflecting it on the calculation of *p-y* curve at

any depth. The CPT-based approach would benefit particularly offshore cases where the process of soil characterization is limited and thus it becomes more important to complement the inherent discontinuous aspect of *p-y* analysis.

Since Kondner (1963) first proposed the hyperbolic function to describe the non-linear soil behavior, it has been widely adopted into various geotechnical problems where the non-linear stress-strain relationship of soils is involved. It reproduces and fits the non-linear stress-strain relationship reasonably well whereas the required model parameters are simpler yet indicating mechanically meaningful correlation to actual soil behavior. The hyperbolic relationship has also been applied to define the *p-y* curve functions (Goh *et al*. 1997, Kim *et al*. 2004, Haldar and Babu 2009).

Following the hyperbolic form, the *p-y* curve can be defined as follows

$$p = \frac{y}{\frac{1}{E_{py,0}} + \beta \cdot \frac{y}{p_u}} \tag{7}$$

where $E_{py,0}$ = initial stiffness on *p-y* curve; p_u = ultimate lateral soil resistance; and β = hyperbolic reduction factor. The parameter β is frequently adopted in the hyperbolic relationship to adjust displacement at failure otherwise infinite displacements are required to reach the ultimate state with an asymptotic value. Introducing the ultimate lateral pile displacement and corresponding *p-y* stiffness, Eq. (7) can be rewritten as the following normalized form

$$\frac{p}{p_u} = \frac{\frac{y}{y_u}}{\alpha + \beta \cdot \frac{y}{y_u}} \tag{8}$$

where y_u = lateral displacement at the ultimate state; α = stiffness ratio = $E_{py,u}/E_{py,0}$; and $E_{py,u}$ = *p-y* stiffness at the ultimate state = p_u/y_u. The stiffness ratio α represents the ratio of initial to ultimate-state *p-y* stiffness.

As the *p-y* stiffness at the ultimate state is related to a strain value at the ultimate state, α can be obtained using the following relationship proposed by Kumar *et al*. (2006)

$$\alpha = 0.052 \cdot \varepsilon_u^{-0.48} \tag{9}$$

where ε_u is a strain value at the ultimate state. According Blaney and O'Neil (1986), ε_u can be obtained from induced lateral displacement of piles at the ultimate state (y_u) and pile diameter D as the following equation

$$\varepsilon_u = \frac{y_u}{1.667D} \tag{10}$$

In Eq. (8), the normalized load p/p_u should be unity at the ultimate state of y/y_u equal to 1. This means that the sum of α and β should also be unity as p/p_u and y/y_u are both equal to 1 at the ultimate state. From Eqs. (9) and (10), the value of α is obtained equal to 0.321 by substituting y_u with 3D/80 that represents displacement at the ultimate state. As α is 0.321, the value of β is

obtained as equal to 0.679. This yields that Eq. (8) is rewritten as

$$\frac{p}{p_u} = \frac{\frac{y}{y_u}}{0.321 + 0.679 \cdot \frac{y}{y_u}} \tag{11}$$

In Eq. (11), p_u is key component that controls calculated lateral pile displacements and load response. p_u represents the maximum lateral soil resistance that can be mobilized for given local soil condition, stress state and strength characteristics of the soil. p_u increases with depth indicating a correlation between p_u and the cone resistance q_c. The direct correlation of the ultimate lateral soil resistance to q_c for laterally loaded piles was first proposed by Lee *et al*. (2010). The CPT-based ultimate lateral soil resistance by Lee *et al*. (2010) can be given by

$$p_u = 2.775 \cdot D \cdot q_c^{0.391} \cdot \sigma_m'^{0.609} \tag{12}$$

where D = pile diameter; q_c = cone resistance; and σ_m' = mean effective stress. Note that Eq. (12) is a modified formulation from the original correlation to maintain the dimensional consistency of p_u in the *p-y* function with a dimensionless normalized form. Using p_u of Eq. (12), the hyperbolic *p-y* function of Eq. (11) can then be rewritten as follows

$$p = q_c^{0.391} \cdot \sigma_m'^{0.609} \frac{y}{0.00434 + 0.245 \cdot \frac{y}{D}} \tag{13}$$

Other than the capability of CPT result utilization, the proposed *p-y* function of Eq. (13) is distinguished from the previous methods in the following aspects: (1) the non-linear load-displacement is described using the hyperbolic function that has been well validated in various soil problems; (2) the effect of horizontal stress, which is known to affect p_u, can be reflected through the mean effective stress term σ_m'; and (3) the proposed method is comparable to the methods currently adopted in design specifications as compared in Fig. 2. Fig. 2 shows the normalized *p-y* curve using Eq. (11), compared with those of Reese *et al*. (1974) and API (2010). It is seen that the *p-y* curves of Reese *et al*. (1974) and API (2010) are quite different while Eq. (11) appears somewhat similar to the *p-y* curve proposed by Reese *et al*. (1974). Note that the lateral load-displacement curves are given in terms of normalized load term p/p_u, actual lateral load-displacement curves may not the same order as shown in Fig. 2.

3.2 Cyclic loading condition

Cyclic loading condition is an important design consideration for offshore structures. To consider the effect of cyclic loading condition in the *p-y* analysis, certain modification factors have been proposed and introduced into the analysis (Reese *et al*. 1974, API 2010, Bienen *et al*. 2012). The modification factor represents the effect of magnifying lateral displacements calculated from the static *p-y* analysis with consideration of number of loading cycles. If the modification factor is set to be multiplied to calculated displacements at pile head, the depth profile of lateral

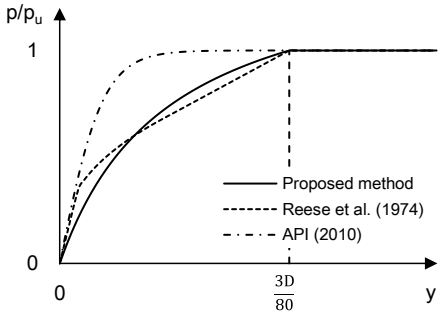

Fig. 2 Comparison of normalized characteristic shapes of *p-y* curves for sand

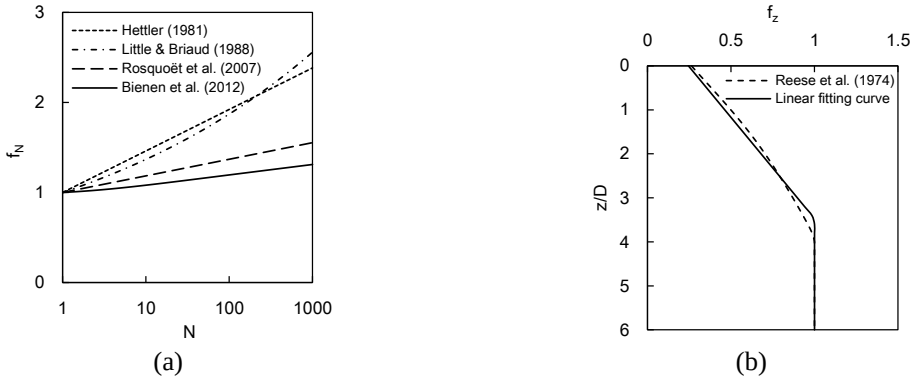

(a) (b)

Fig. 3 Cyclic factors for analysis of pile under lateral loading

displacements under cyclic loading condition or cyclic *p-y* curve is not known. Fig. 3(a) shows examples of such modification factor (f_N) proposed by different authors.

Bienen *et al*. (2012) proposed a lateral displacement modification factor that can take into account the cyclic accumulation effect given as follows

$$f_N = 1 + 0.05 \cdot \frac{N-1}{N} \cdot \left[LN(0.5N) + 1\right] \tag{14}$$

where f_N = modification factor for cyclic loading condition; and N = number of loading cycles. As compared in Fig. 3(a), Eq. (14) produces lower magnifying effect than those of Hettler (1981), Little and Briaud (1988) and Rosquoët *et al*. (2007). For the number of loading cycles equal to 1000, the value of f_N from Eq. (14) was equal to 1.31 indicating 31% increase in lateral displacement compared to static loading condition. The values of f_N from Hettler (1981) and Little and Briaud (1988) were similar.

According to Reese *et al*. (1974), the effect of cyclic loading on the *p-y* curve is most significant at surface and decreases with depth. It was presented that the effect of cyclic loading becomes negligible below depths of 3 to 3.5 time pile diameter D. For the *p-y* curve under cyclic loading, a fitting equation based on the empirical adjustment parameters proposed by Reese *et al*. (1974) was obtained given as follows

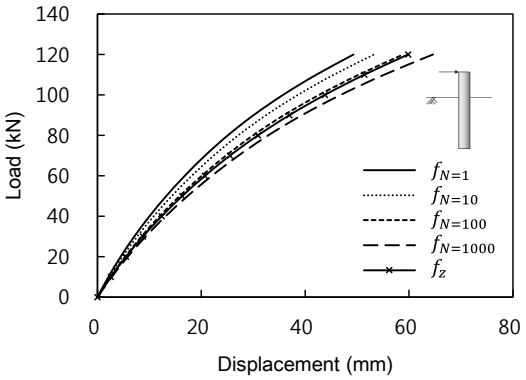

Fig. 4 Comparison of lateral load-displacement curves with different cyclic factor of f_N and f_z

$$f_z = 0.2175 \cdot \left(\frac{z}{D}\right) + 0.245 \tag{15}$$

where z = depth and D = pile diameter. The depth variation of f_z from Eq. (15) and Reese *et al*. (1974) are compared in Fig. 3(b). Note that the number of loading cycles is not included in Eq. (15) as it was assumed that the effect of cyclic loading condition becomes constant after a certain number of loading cycles. While Eq. (14) is only applied to pile-head displacements, Eq. (15) is multiplied directly to the *p-y* function implying that bending moment, shear force and soil reaction under cyclic loading condition can all be obtained over the depth of the pile. Consequently, Eq. (15) was multiplied to the proposed *p-y* equation of Eq. (13) to obtain cyclic lateral load-displacement curves.

To compare the two different approaches describe above, Eqs. (14) and (15) were adopted into the proposed *p-y* analysis and calculated lateral load responses were compared. Fig. 4 compares the load-pile head displacement curves obtained using f_N of Eq. (14) and f_z of Eq. (15) for a given soil and pile condition. The soil and pile properties used in Fig. 4 will further be described in next section. It is seen that the load-displacement curve obtained using f_z of Eq. (15) is similar to the result using f_N of Eq. (14) with the number of loading cycles equal to 100.

3.3 Implementation for load transfer analysis

The proposed *p-y* analysis method was coded and implemented through the load transfer analysis algorithm based on the beam on elastic foundation model. For the beam-on-elastic foundation model, the governing differential equation for the equilibrium condition of a pile segment is given by

$$E_p I_p \frac{d^4 y}{dz^4} + Q\frac{d^2 y}{dz^2} - p + W = 0 \tag{16}$$

where E_pI_p = flexural rigidity of pile; Q = axial load; p = soil reaction per unit length; and W = distributed load along pile. Applying the finite difference scheme, the governing differential equation of Eq. (16) can be written as the following discretized form

$$a_i \cdot y_{i-2} + b_i \cdot y_{i-1} + c_i \cdot y_i + d_i \cdot y_{i+1} + e_i \cdot y_{i+2} = f_i \tag{17}$$

where *a*, *b*, *c*, *d*, *e*, and *f* are model coefficients. The subscript *i* represents the node number of discretized pile segments. Model coefficients included in Eq. (17) are determined from the system equations established for the assigned nodes on pile segments that are characterized by the flexural rigidity of pile (EI) and soil spring stiffness given by the *p-y* curves.

In a matrix form, the governing equation of Eq. (17) can be given as follows

$$[A] \cdot (y) = (f) \tag{18}$$

where [*A*] = stiffness matrix; (*y*) = lateral displacement vector matrix; and (*f*) = load vector matrix.

The load transfer mechanism and the proposed CPT-based *p-y* analysis method described herein were coded using the commercial programing software MATLAB. Fig. 5 shows the calculation algorithm and steps for the load transfer analysis using the proposed *p-y* curve method.

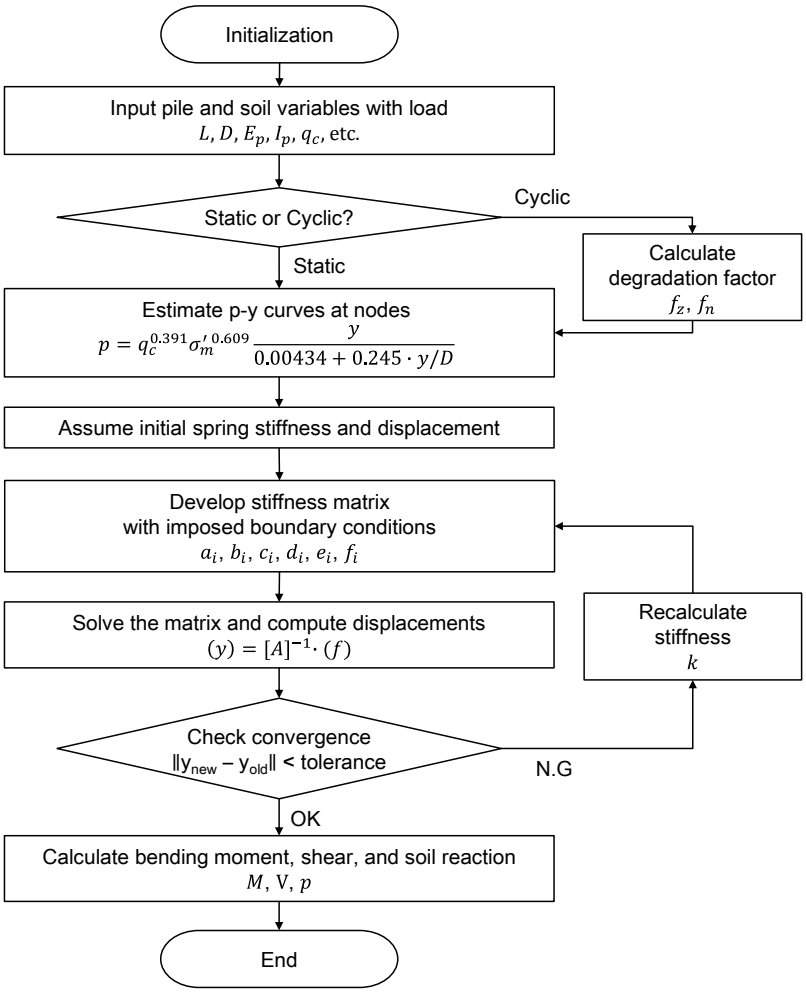

Fig. 5 Calculation algorithm

4. Comparison with case examples

4.1 Static loading case

A case example, which contains results from lateral pile load test and CPT, was selected from the literature (Rollins *et al*. 2005) and used to check the validity of the proposed method. The test site was located at National Geotechnical Experiment Site (NGES) on Treasure Island in San Francisco Bay, US. The soils at the test site were predominantly sands down to the depth of 7.5 m below which a 1.8-m clay layer existed. The upper sand layers down to the 7.5-m depth were classified into SP, SP-SM, and SM according to the Unified Soil Classification System (USCS). The detailed soil layering condition is shown in Fig. 6(a). The cone penetration test was conducted and the depth profile of cone resistance (q_c) is given in Fig. 6(b). It is seen that the majority of q_c values are in the range between 4 to 9 MPa. More detailed property condition of the soils at the test site is given Table 1. For the values of internal friction angle (ϕ'), different methods of API (2010) and Bolton (1986) were used as reported in Rollins *et al*. (2005). These are both included in Table 1. As compared in the table, higher values of ϕ' were estimated from Bolton's method as the values of ϕ' by Bolton's method include the dilatancy friction angle that represents the state-dependent strength mobilized at peak strength state.

The friction angle for API's method is given as following equations

$$\phi = 16D_R^2 + 0.17D_R + 28.4 \tag{19}$$

where ϕ = internal friction angle and D_R = relative density (as a number between 0 and 1).

For Bolton's method, the following dilatancy equations were used

$$\phi_p = \phi_c + 3I_R \tag{20}$$

$$I_p = D_R\left[Q - \ln\left(\frac{100\sigma'_{mp}}{p_A}\right)\right] - R \tag{21}$$

where ϕ_p = peak friction angle; ϕ_c = critical-state friction angle; I_R = dilatancy index; D_R = relative density (as a number between 0 and 1); p_A = reference stress = 100 kPa; σ'_{mp} = mean effective stress; and Q and R = intrinsic soil variables.

The test pile was made of open-ended steel pipe with an outside diameter equal to 0.324 m and a thickness of 0.0095 m. The embedded pile length was 11.5 m with the vertical load eccentricity above the ground surface equal to 0.69 m. The elastic modulus (E) and the 2nd moment of inertia (I) of the test pile were 200 GPa and 0.000116 m^4, respectively.

The *p-y* analyses were performed for the selected case example using different prediction methods including the proposed CPT-based method and those of Reese *et al*. (1974), API (2010), Novello (1999), and Suryasentana and Lehane (2014), all of which were described previously. For the cases using API's and Reese *et al*.'s methods, the two different friction angles were adopted in the analysis and compared with measured results. For the clay layer, the existing method by Matlock (1970) was used.

Fig. 7 shows measured and calculated load versus pile head displacement for different prediction methods. It is seen that the calculated load-displacement curve using the proposed

Table 1 Summary of soil properties for static *p-y* analysis (Treasure Island)

z[1] (m)	Soil type	γ_{sat}[2] (kN/m^3)	s_u[3] (kPa)	ϕ[4] (deg.)		k[5] (MN/m^3)		ε_{50}[6]
				API	Bolton	API	Bolton	
0.00 ~ 0.51	Sand	19.5 (not saturated)	-	33	39	24.4	60.0	-
0.51 ~ 2.59	Sand	20.1	-	33	39	15.4	35.2	-
2.59 ~ 2.97	Sand	20.1	-	32	37	13.6	35.2	-
2.97 ~ 3.99	Sand	20.1	-	32	36	13.6	29.8	-
3.99 ~ 4.73	Sand	20.1	-	32	36	13.6	24.4	-
4.73 ~ 6.00	Sand	20.1	-	30	36	10.8	24.4	-
6.00 ~ 7.49	Sand	20.1	-	30	35	10.8	21.7	-
7.49 ~ 9.25	Soft clay	19.3	19.2	-	-	-	-	0.01
9.25 ~ 10.16	Sand	20.1	-	30	34	10.8	19.0	-
10.16 ~ 11.84	Soft clay	19.3	19.2	-	-	-	-	0.01

[1] z: Depth, [2] γ_{sat}: Saturated unit weight, [3] s_u: Undrained shear strength,
[4] ϕ: Friction angle, [5] k: Lateral subgrade modulus, [6] Characteristic strain

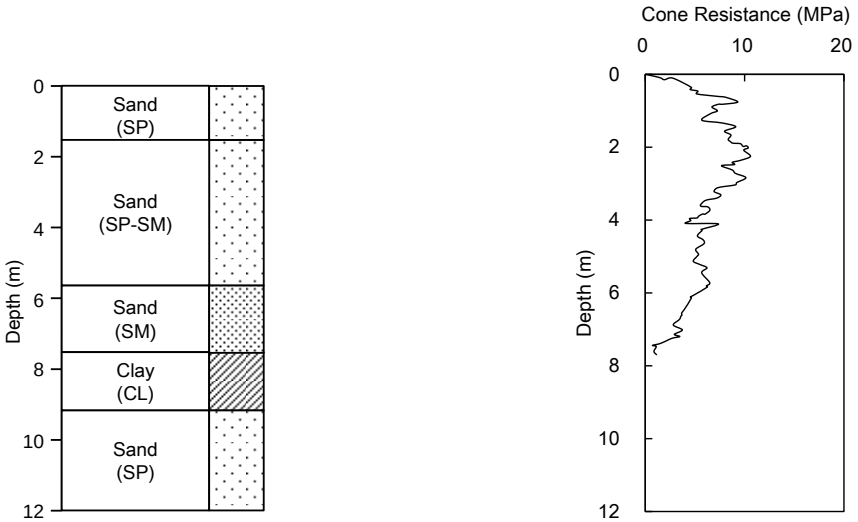

(a) Soil profile (b) CPT profile

Fig. 6 Soil profiles at test site in Treasure Island (Rollins *et al*. 2005)

CPT-based method match well the measured results. The CPT-based methods by Novello (1999), and Suryasentana and Lehane (2014) also produced reasonable match to the measured results while underestimated displacements were produced from Dyson and Randolph (2001).

For the methods of API (2010) and Reese *et al*. (1974), the accuracy of calculated results was quite different depending on the values of friction angle. As the Bolton's friction angles in Table 1 are higher due to the consideration of dilatancy angle, the calculated results also show stiffer load

responses. For this case example, the friction angle from Bolton's method showed better match to the measured results. Note that no selection of friction angle is necessary for the CPT-based methods as the cone resistance itself represents strength characteristics of the soil. The difference in input soil parameters for each method results in different values of calculated load with different tendency from that shown in Fig. 2.

Measured and calculated bending moment profiles along the pile are shown in Fig. 8 for the two different loading levels of lateral load H = 24.0 and 89.0 kN. For API's and Reese *et al*.'s methods, the friction angles from Bolton's methods were used. At H = 24.0 kN, it is seen that all prediction methods underestimated the values of mobilized bending moment. At higher load level of H = 89.0 kN, closer match was observed between the measured and calculated results. Overall, the calculated bending moment profiles, including magnitude and depth to the maximum bending moment, were in good agreement with the measured profiles.

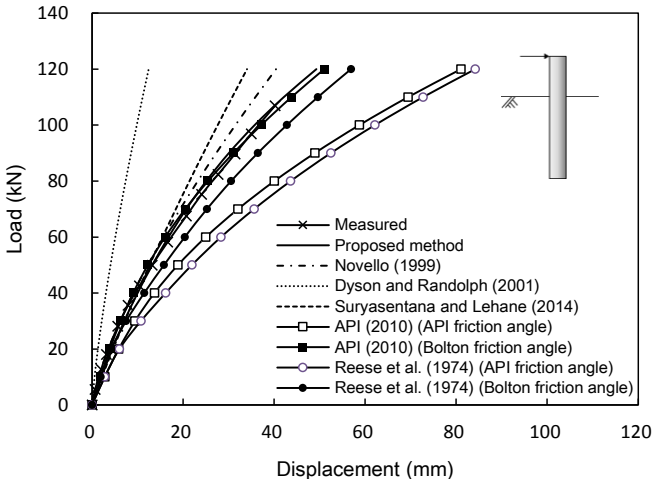

Fig. 7 Load versus pile head displacement curves

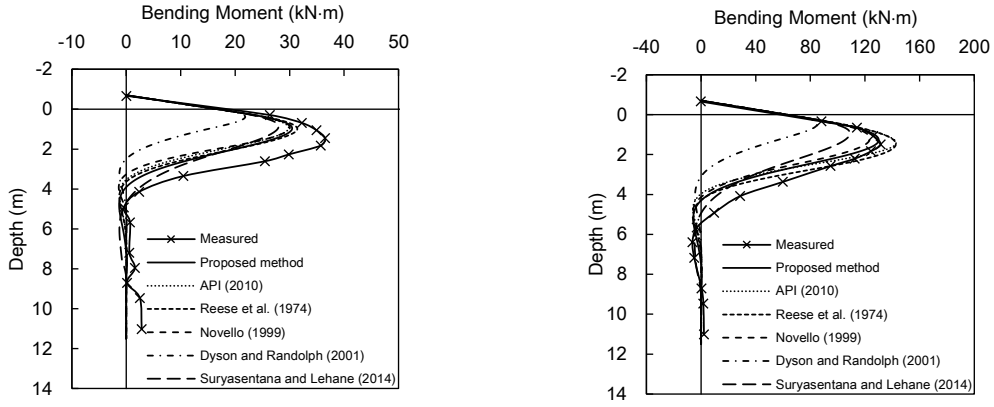

(a) Applied load = 24.0 kN (b) Applied load = 89.0 kN

Fig. 8 Depth versus bending moment curves at two loading levels

4.2. Cyclic loading case

Additional case example was selected from the literature to check and compare calculated and measured load responses under cyclic loading condition. The selected example was the centrifuge tests for cyclic loading condition conducted by Rosquoët *et al*. (2007). The centrifuge tests were conducted at the centrifuge acceleration of 40 g. The test pile was 0.72 and 12 m in diameter and length, respectively, with bending stiffness (EI) equal to 476 MN·m^2. The one-way cyclic load of 960 kN was applied at 1.6 m above the ground surface. For the test specimens, the relative density (D_R), unit weight (γ') and friction angle (ϕ') of the soil were 86%, 15.99 kN/m^3 and 41°, respectively. The cone penetration test was conducted and the depth profile of the cone resistance is shown in Fig. 9. The CPT profile follows the linear fitting equation given as follows

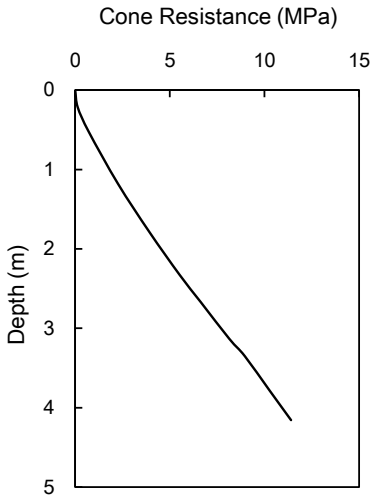

Fig. 9 CPT profile of test sand at D_R = 86%, (Rosquoët *et al*. 2007)

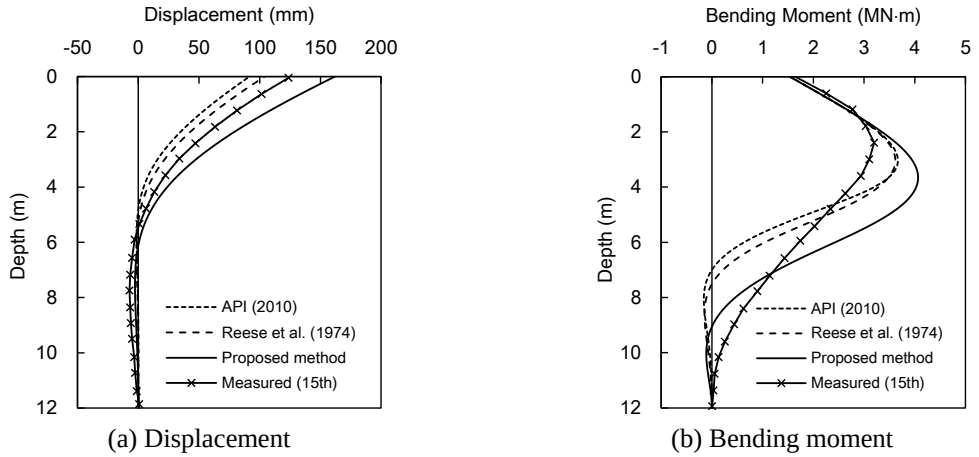

(a) Displacement (b) Bending moment

Fig. 10 Comparison of measured and computed result versus depth curves for 15th cycle

$$q_c \approx 3z \tag{22}$$

The measured results were obtained for the loading cycles (N) of 15 and these results were adopted in the comparison. Measured and calculated depth-lateral displacement curves under cyclic loading conditions are shown in Figs. 10(a). Note that, for the calculation in Fig. 10, the cyclic modification factors f_z of Eq. (15) was adopted in the proposed CPT-based method. From Fig. 10(a), it is seen that the result from Reese *et al.*'s method showed the best fit to the measured values. The proposed method produced slightly overestimated results, which may be due to the difference of the numbers of loading cycles considered in the proposed method. Fig. 10(b) shows the depth distribution of mobilized bending moment along pile. Differently from the static case, the profiles of calculated bending moments showed somewhat overestimated results with deeper depths to the maximum bending moment than measured depth due to the difference of the number of cycles as the result of displacement curve in the *p-y* analysis approach for cyclic loading conditions.

6. Conclusions

The lateral load response is key design consideration for offshore mono-piles as waves and winds are predominant load components. In this study, a CPT-based *p-y* analysis method was proposed to evaluate the lateral load responses of offshore mono-piles embedded in sands. Both static and cyclic loading conditions were considered in the proposed method. The main goal of this study is to develop a *p-y* analysis method that can utilize the results from CPT, which is particularly effective for offshore soil characterization. The continuous soil profiling capability of CPT is an important consideration for the proposed method, where detailed depth variation of soil profiles can be readily incorporated into the analysis using CPT results.

The hyperbolic function was adopted to describe the non-linear *p-y* curves as it can relate an imposed lateral load directly to pile displacement with simpler model parameters in a straightforward manner. The hyperbolic model parameters were evaluated based on the ratio of initial to ultimate state *p-y* stiffness. For the proposed hyperbolic *p-y* relationship, the ultimate lateral soil resistance p_u is key component that was obtained introducing the correlation of the ultimate lateral resistance to the cone resistance. The CPT-based *p-y* function of Eq. (13) was adopted into the load transfer analysis for laterally loaded pile and estimation of displacement analysis where a CPT depth profile of cone resistance is directly introduced as an input resource. For cyclic loading condition, the cyclic modification factor, given as a function of loading cycle, and depth variation profile of cyclic loading effect was incorporated into the proposed CPT-based *p-y* curve function. The load transfer analysis algorithm using the proposed *p-y* functions for both static and cyclic loading conditions was coded using MATLAB and used in the analysis.

Case examples that contain lateral pile load test results were selected from the literatures to check the validity of the proposed CPT-based method. For the static loading case, it was seen that the calculated results using the proposed CPT-based method match surprisingly well the measured results. For the existing methods, the accuracy of calculated results was quite different depending on the values of friction angle adopted into the analysis. The profiles of calculated bending moment, including magnitude and depth to the maximum bending moment, also showed reasonable agreement with the measured profiles. For cyclic loading condition, the proposed method showed reasonable agreement with measured displacement profiles. The calculated

profiles of bending moment profiles were however somewhat overestimated with deeper depths to the maximum bending moment than measured depth.

Acknowledgments

This work was supported by Basic Science Research Program through the National Research Foundation of Korea (NRF) grants funded by the Korean government (MSIP) (Nos. 2011-0030040 and 2013R1A1A2058863)

References

American Petroleum Institute, API. (2010), *Recommended Practice for Planning, Designing and Constructing Fixed Offshore Platforms - Working Stress Design*, API Recommended Practice 2A-WSD (RP2A-WSD), (21st Edition), API Publishing Services, Washington D. C.

Bienen, B., Dührkop, J., Grabe, J., Randolph, M.F. and White, D.J. (2012), "Response of piles with wings to monotonic and cyclic lateral loading in sand", *J. Geotech. Geoenviron. Eng., ASCE*, **138**(3), 364-375.

Blaney, G.W. and O'Neill, M.W. (1986), "Measured lateral response of mass on single pile in clay", *J. Geotech. Eng., ASCE*, **112**(4), 443-457.

Briaud, J.L., Tucker, L., Lytton, R.L. and Coyle, H.M. (1985), "Behavior of piles and pile groups in cohesionless soils", Final Report, Report No. FHWA/RD-83/038, NTIS PB86-152089/AS.

Chang, B.J. and Hutchinson, T.C. (2013), "Experimental evaluation of *p-y* curves considering development of liquefaction", *J. Geotech. Geoenviron. Eng., ASCE*, **139**(4), 577-586.

Det Norske Veritas, DNV. (2013), *Design of Offshore Wind Turbine Structures*, Offshore Standard DNV-OS-J101.

Dyson, G.J. and Randolph, M.F. (2001), "Monotonic lateral loading of piles in calcareous sand", *J. Geotech. Geoenviron. Eng., ASCE*, **127**(4), 346-352.

Franke, K. and Rollins, K. (2013), "Simplified hybrid *p-y* spring model for liquefied soils", *J. Geotech. Geoenviron. Eng., ASCE*, **139**(4), 564-576.

Gabr, M., Lunne, T. and Powell, J. (1994), "*P-y* analysis of laterally loaded piles in clay using DMT", *J. Geotech. Eng., ASCE*, **120**(5), 816-837.

Goh, A.T.C., Teh, C.I. and Wong, K.S. (1997), "Analysis of piles subjected to embankment induced lateral soil movements", *J. Geotech. Geoenviron. Eng., ASCE*, **123**(9), 792-801.

Haldar, S. and Babu, G.S. (2009), "Design of laterally loaded piles in clays based on cone penetration test data: a reliability-based approach", *Géotechnique*, **59**(7), 593-607.

Hettler, A. (1981), "Verschiebungen starrer und elastischer Gründungskörper in Sand bei monotoner und zyklischer Belastung." ph.D. Dissertation, University of Karlsruhe, Karlsruhe.

Khalili-Tehrani, P., Ahlberg, E.R., Rha, C., Lemnitzer, A., Stewart, J.P., Taciroglu, E. and Wallace, J.W. (2014), "Nonlinear load-deflection behavior of reinforced concrete drilled piles in stiff clay", *J. Geotech. Geoenviron. Eng., ASCE*, **140**(3), 04013022.

Kim, B.T., Kim, N.K., Lee, W.J. and Kim, Y.S. (2004), "Experimental load–transfer curves of laterally loaded piles in nak-dong river sand", *J. Geotech. Geoenviron. Eng., ASCE*, **130**(4), 416-425.

Kondner, R.L. (1963), "Hyperbolic stress-strain response of cohesive soils", *J. Soil Mech. Found. Div., ASCE*, **89**(1), 115-143.

Kumar, S., Lalvani, L. and Omar, M. (2006), "Nonlinear response of single piles in sand subjected to lateral loads using k_{hmax} approach", *Geotech. Geol. Eng.*, **24**(1), 163-181.

Lee, J. and Randolph, M. (2011), "Penetrometer-based assessment of spudcan penetration resistance", *J. Geotech. Geoenviron. Eng., ASCE*, **137**(6), 587-596.

Lee, J.H. and Salgado, R. (1999), "Determination of pile base resistance in sands", *J. Geotech. Geoenviron.*

Eng., **125**(8), 673-683.
Lee, J., Eun, J., Lee, K., Park, Y. and Kim, M. (2008), "In-situ evaluation of strength and dilatancy of sands based on CPT results", *Soil Found*., **48(**2), 255-266.
Lee, J., Kim, M. and Kyung, D. (2010), "Estimation of lateral load capacity of rigid short piles in sands using CPT results", *J. Geotech. Geoenviron. Eng*., *ASCE*, **136**(1), 48-56.
Little, R.L. and Briaud, J.L. (1988), "Full scale cyclic lateral load tests on six single piles in sand", Miscellaneous Paper GL-88-27; Geotechnical Div., Texas A&M University, College Station, TX, USA.
Matlock, H. (1970), "Correlation for design of laterally loaded piles in soft clay", *Proceedings of the 2nd Annual Offshore Technology Conference*, OTC, Houston, TX, USA, April, pp. 577-594.
Matlock, H. and Reese, L.C. (1960), "Generalized solutions for laterally loaded piles", *J. Soil Mech. Found*., *ASCE*, 86(5), 63-91.
McGann, C.R., Arduino, P. and Mackenzie-Helnwein, P. (2011), "Applicability of conventional *p-y* relations to the analysis of piles in laterally spreading soil", *J. Geotech. Geoenviron. Eng*., *ASCE*, **137**(6), 557-567.
Novello, E.A. (1999), "From static to cyclic *p-y* data in calcareous sediments", *Proceedings of Engineering for Calcareous Sediments*, Balkema, Rotterdam, The Netherlands.
Pando, M., Ealy, C., Filz, G., Lesko, J. and Hoppe, E. (2006), "A Laboratory and Field Study of Composite Piles for Bridge Substructures", Report FHWA-HRT-04-043; FHWA.
Reese, L.C. (1997), "Analysis of laterally loaded piles in weak rock", *J. Geotech. Geoenviron. Eng*., *ASCE*, **123**(11), 1010-1017.
Reese, L.C., Cox, W.R. and Koop, F.D. (1974), "Analysis of laterally loaded piles in sand", *Proceedings of the 6th Annual Offshore Technology Conference*, OTC, Houston, TX, USA, May, pp, 473-485.
Reese, L.C., Cox, W.R. and Koop, F.D. (1975), "Field testing and analysis of laterally loaded piles in stiff clay", *Proceedings of the 7th Offshore Technology Conference*, OTC, Houston, TX, USA, May, pp. 671-690.
Rix, G.J. and Stokoe, K.H. (1991), "Correlation of initial tangent modulus and cone penetration resistance", *Proceedings of the 1st International Symposium on Calibration Chamber Testing*, Potsdam, NY, USA, June, pp. 351-362.
Robertson, P.K. and Campanella, R.G. (1983), "Interpretation of cone penetration tests I: sand", *Can. Geotech. J*., **109**(11), 1449-1459.
Robertson, P.K., Davis, M.P. and Campanella, R.G. (1989), "Design of laterally loaded driven piles using the flat dilatometer", *Geotech. Test. J*., **12**(1), 30-38.
Rollins, K.M., Lane, J.D. and Gerber, T.M. (2005), "Measured and computed lateral response of a pile group in sand", *J. Geotech. Geoenviron. Eng*., *ASCE*, **131**(1), 103-114.
Rosquoët, F., Thorel, L., Garnier, J. and Canepa, Y. (2007), "Lateral cyclic loading of sand-installed piles", *Soil. Found*., **47**(5), 821-832.
Schnaid, F. and Houlsby, G.T. (1991), "An assessment of chamber size effects in the calibration of in situ tests in sand", *Géotechnique*, **41**(3), 437-445.
Suryasentana, S. and Lehane, B.M. (2014), "Numerical derivation of CPT-based *p-y* curves for piles in sand", *Géotechnique*, **64**(3), 186-194.
Titi, H.H., Mohammad, L.N. and Tumay, M.T. (2000), "Miniature cone penetration tests in soft and stiff clays", *Geotech. Test. J*., *ASTM*, **23**(4), 432-443.
Tumay, M.T. and Kurup, P.U. (2001), "Development of a continuous intrusion miniature cone penetration test system for subsurface explorations", *Soil. Found*., **41**(6), 129-138.
Winkler, E. (1867), *Die Lehre von der Elastisitat und Festigkeit*, Dominicus, Prague, Czech Republic.

GC